TELKOMNIKA, Vol.16, No.3, June 2018, pp. 1092~1100
ISSN: 1693-6930, accredited **A** by DIKTI, Decree No: 58/DIKTI/Kep/2013
DOI:10.12928/TELKOMNIKA.v16i3.7722

Lowpass Filter with Hilbert Curve Ring and Sierpinski Carpet DGS

Dian Widi Astuti*, Intan Wahyuni, Muslim, Mudrik Alaydrus
Department of Electrical Engineering, Universitas Mercu Buana
Jl. Meruya Selatan No 1 Jakarta Barat, 5840816
*Corresponding author, e-mail: dian.widiastuti@mercubuana.ac.id

Abstract

Good performance and compact size are the paramaters which are vital when desiging a filter. One of the creteria of good performance is selectivity. This research, conducted by Hilbert Curve Ring and Siepinski Carpet, is used as defected ground structure to overcome filter selectivity. By using three cascadeds Hilbert Curve Ring defected ground structure cells and three steps Sierpinski carpet, a lowpass filter is designed and fabricated. The measurement result for lowpass filterwith Hilbert Curve Ring defected ground structure has sharper selectivity with the cut off frequency at 2.173 GHz and the insertion loss value is 2.135 dB. While the measurement result for three steps Sierpinski carpet has the cut off frequency at 1.728 GHz and the insertion loss value is 0.682 dB.

Keywords: *Lowpass filter, defected ground structure, hilbert curve ring, sierpinski carpet, microstrip filter*

1. Introduction

In telecommunication systems, a filter plays a very important role in selecting which information to be used or to be rejected. There are many types of filters, for example bandpass filter, dualband bandpass filter, highpass filter, lowpass filter and many more. A lowpass filter rejects signals which have higher frequency than the cut-off frequency. A lowpass filter, if connected behind a bandpass filter can discard multiple resonant frequencies, which is not rejected by the bandpass filter.A relatively simple method of realizing the lowpass filter is the stepped-impedance. The stepped-impedance contains high-impedance and low-impedance microstrip to model inductor and capacitor. However the the selectivity of the filteris still sloping to reduce the interferences. A sharp selectivity is very important in producing a filter. The sharp selectivity can be improved by using two coupled resonators and source-load coupledto generate transmission zeros [1-3]. Another important aspect in filter design is the filter dimension. A compact size of filter realization can be achieved by decreasing the number of resonators, using via ground holes technique and using substrate that has higher dielectric constant [4] or using a rectangular resonator sandwiched between two interdigital structures, [5]. Moreover, it can also be improved by defected ground structure. Having a simple structure, defected ground structure is equivalent to L-C circuit model, and has extensive applicability to design couplers, power divider, amplifiers and filters [6-9].

An etched defect in ground plane disturbs the current distribution in the ground plane, called defected ground structure (DGS). This disturbance can change the characteristics of a transmission line such as line capacitance and inductance. The low-pass filter using the DGS circuit has a number of attractive features, which include the following: very simple, wider and deeper the stopband than the conventional low-pass filter, very low insertion loss and extremely small element values for implementation of low-pass filter which can be realized [10].

The DGS design model evolved from a simple dumb-bell square shaped [11-13], elliptic [14], split-ring resonator [15], "H" shape slots [16], combination between spiral-shaped and dumb-bell shaped [17, 18], meander [19], Hilbert Curve Ring [20-22] in order to obtain narrower bandpass region or a sharper skirt selectivityof filter. Hilbert Curve Ring is one of the fractal geometries besides Sierpinski Carpet or Gasket, Koch curve and Cantor.Fractal geometries are different from Euclidean geometries which havetwo unique properties such as space-filling and self-similarity like array techniques. They have been used widely in RF and microwave applications such as antennas [23-29] besides array techniques [30-33]. They can

Received November 2, 2017; Revised February 24, 2018; Accepted March 10, 2018

also be used in filter applicationsthat it presented in [34-36], to reduce resonant frequency of the structure and to achieve improved frequency selectivity in the resonator performance. Moreover, fractal geometries offer smaller resonator size.

This research presentsthe selectivity improvement of stepped-impedance lowpass filter by using Hilbert Curve Ring and Sierpienski Carpet as defected ground structure.Generally, Sierpinski Carpet is used for antenna applications to minimize antenna sizes, develop multiband [24], eliminate the harmonics frequencies of the higher order modes [25] and harvesting applications [29]. Sierpinski Carpetcan also be applied for filter applications but not as a defected ground structure [32].

2. Design and Analysis of Hilbert Curve Ring Lowpass Filter

Figure 1a shows the lowpass filter design with Hilbert Curve Ring defected ground structure. Figure 1b shows the top layer of the Chebyshev Stepped-Impedance lowpass filter design, whereas the equivalent circuit of the lowpass filter is depicted in Figure 1c.

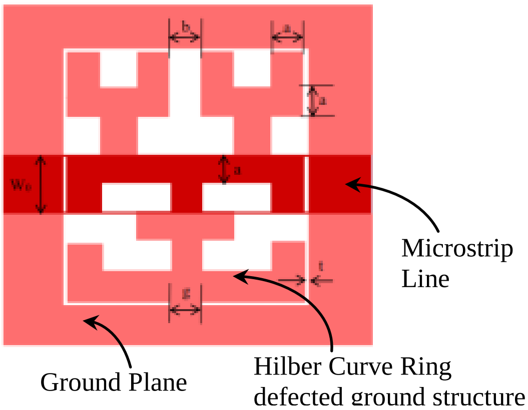

(a)

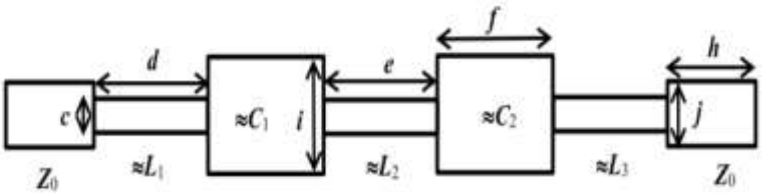

(b)

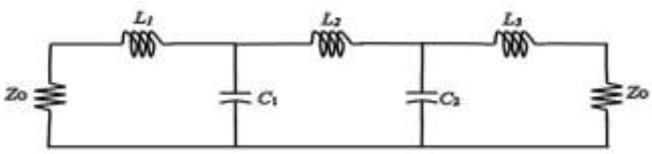

(c)

Figure 1. The lowpass filter design with Hilbert Curve Ring defected ground structure (a), the Hilbert Curve Ring defected ground structuredesign at the bottom of lowpass filter, (b) The top layer of the lowpass filter design (c) The equivalent circuit of lowpass filter

The governing equations for designing the lowpass filter are given by [37]:

$$\omega_C L = Z_{0L} \sin\left(\frac{2\pi l_L}{\lambda_{gL}}\right) \Rightarrow l_L = \frac{\lambda_{gL}}{2\pi} \sin^{-1}\left(\frac{\omega_C L}{Z_{0L}}\right) \quad (1)$$

$$\omega_C C = \frac{1}{Z_{0C}} \sin\left(\frac{2\pi l_C}{\lambda_{gC}}\right) \Rightarrow l_C = \frac{\lambda_{gC}}{2\pi} \sin^{-1}\left(\omega_C C Z_{0C}\right) \quad (2)$$

where, Z_{0C} and Z_{0L} denote the characteristic impedance of the low and high impedance lines, respectively, and Z_0 is the source impedance, which is usually chosen to 50 ohms. The physical lengths of the low- and high-impedance are l_C and l_L, while λ_g is guided wavelength of the quasi-TEM mode of microstrip.

A substrate RT duroid 5870 with a relative dielectric constant (ε_r) of 2.33, thickness 0.787 mm (0.031 inch) and dissipation factor, tan δ of 0.0012 is chosen in this research. By using the Sonnet simulator, we simulate width and length of c, *d*, *e* of the lowpass filter while another parameter of Hilbert Curve Ring defected ground structure design remains *a*=1.2 mm, *b*=1 mm, split-gap, *g*=1 mm and ring-width *t*=0.4 mm are constant.

Figure 2 shows the simulation resultfor two width value of the inductor, *c*, where*d*=7.1 mm, *e*=13.9 mm, *f*=14.4 mm, *h*=10 mm, *i*=3.5 mm, *j*=2.3are fixed. If *c*has a width of 0.9 mm then the simulation result is obtained the cut-off frequency at 3 dB is 2.088 GHz. While if the width of c is widened to 1.5 mm then the cut-off frequency becomes 2.48 GHz. It means if *c* is widened, the cut-off frequency will shift to the higer frequency.

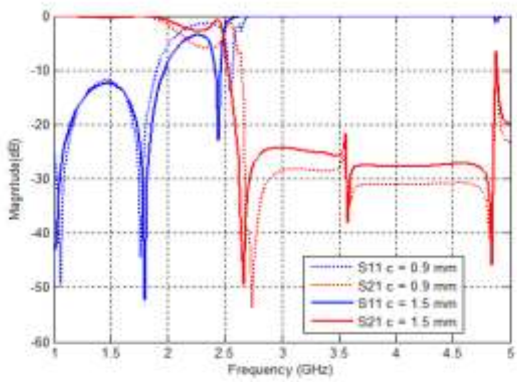

Figure 2. The simulation result by the width variation of *c* (Value of high impedance)

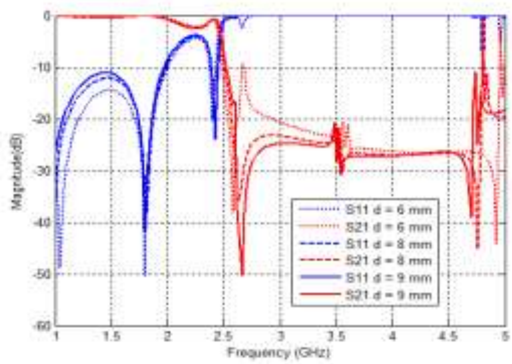

Figure 3. The simulated results of Hilber Curve Ring defected ground structure with several lengths of *d* (length of high impedance line)

Figure 3 shows the simulated results of Hilbert Curve Ring defected ground structure with several lengths of *d*. It can be seen that if the length of *d* is shortened from 9 mm to 6 mm then after the selectivity of the lowpass filter isn't sharp and it shows spurius frequency. While the good simulation happened at *d*=9 mm with the largest insertion loss value is 50.3265 dB at a frequency 2.66 GHz.

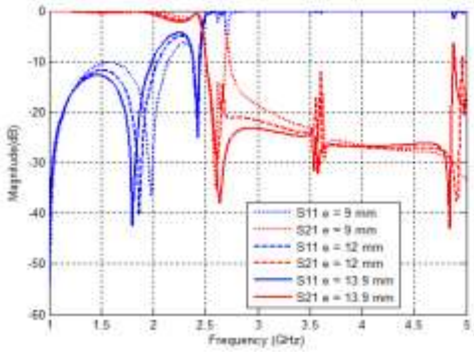

Figure 4. The simulation result by length variation of *e* (length of low impedance line)

Parameter study of *e* the HCR DGS lowpass filter design was performed. The simulation is done by shortening the length of *e*from 13.9 mm to 12 mm and 9 mm, where *d* is7.1 mm. The simulation result is shown in Figure 4. From Figure 4 it is seen that if the length of the *e* resonator is shortened from 13.9 mm to 9 mm then it will form a harmonic frequency resulting in a less selective filter characteristics.It can be concluded that the parameter *d* and *e* will influence the harmonic or spurius frequency while the parameter of *c* will control the cut-off frequency, insertion loss and return loss either.

3. Sierpinski Carpet Lowpass Filter Design

Figure 5 shows various DGS of the Sierpinski Carpet designs. Figure 5*a* is for 2 steps of the Sierpinski Carpet while the copper layer is etched, Figure 5*b* is the opposite of Figure 5*a.* Figure 5*c* and 5*d* is for 3 steps of the Sierpinski carpet, Figure 5*d* is the opposite of Figure 5*c*, the copper layer is shown by the red color. The parameter of the Sierpinski carpet defected ground structure are *k*=1.2 mm, *l*=2.4 mm, *m*=3.6 mm, *n*=0.4 mm, *o*=0.8 mm and *Wo*=1.2 mm, whille the top of lowpass filter design are *c*=Wo=1.2 mm, *d*=6 mm, *e*=11 mm, *f*=14.4 mm *h*=10 mm, *i*=3.5 mm and *j*=2.3 mm.

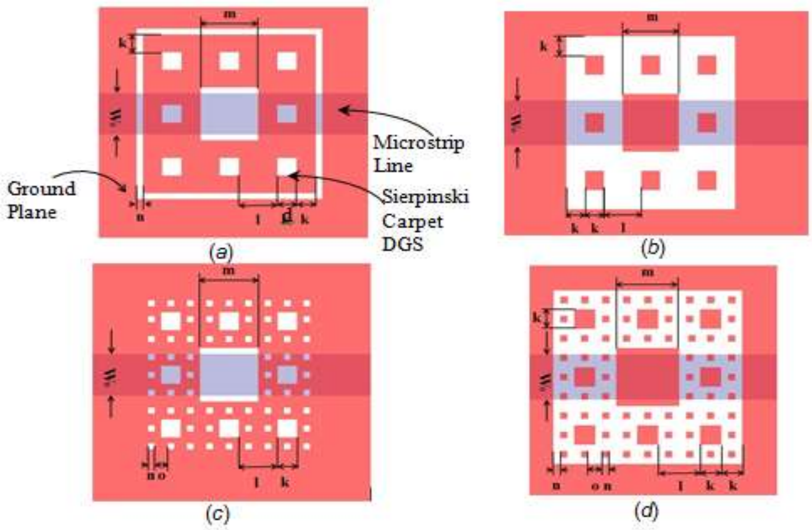

Figure 5. Various designs for Sierpinski Carpet DGS LPF, (*a*) The 2 steps of Sierpinski Carpet, (*b*) the opposite of Figure 5*a.* (*c*) The 3 steps of Sierpinski Carpet, (*d*) the opposite of Figure 5*c*

4. Prototype and Measurement of Lowpass Filter

Figure 6 shows the fabrication of each Hilbert Curve Ring and Sierpinski Carpet defected ground structure. Figure 6*a* is the top layer of lowpass filter with Hilbert Curve Ring defected ground structure, while Figure 6*b* is bottom layer of Hilbert Curve Ring defected ground structure. Figure 6*c* is the top layer of each lowpass filter with Sierpinski Carpet defected ground structure, while Figure 6*d*, *e*, *f*, and *g* are the bottom layer of each various design lowpass filter Sierpinski Carpet defected ground structure.

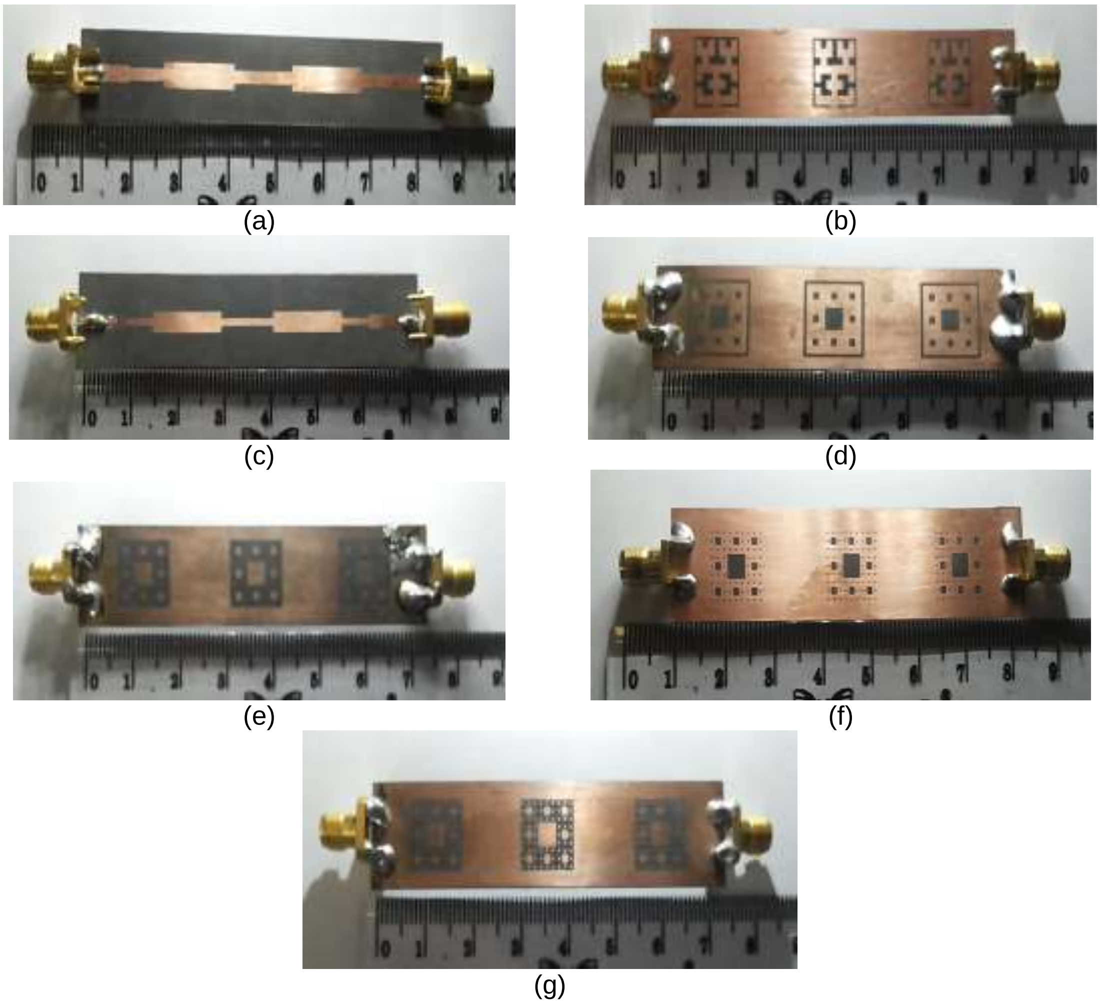

Figure 6. The realization of DGS LPF, (*a*) the top layer of HCR DGS LPF, (*b*) the bottom layer of HCR DGS LPF, (*c*) the top layer of each Sierpinski carpet DGS LPF, (*d*-*g*) the bottom layer of Sierpinski carpet DGS LPF

Figure 7 gives the simulation and measurement result of HCR DGS LPF. From Figure 7, we can see the discrepancy frequency from higher frequency to the lower frequency. The discrepancy frequency is around 180 MHz. From the simulation result, the cut off frequency is at 2.42 GHz and the insertion loss is 0.6616 dB. While the measurement result shows that the cut off frequency is at 2.173 GHz with the insertion loss value at 2.135 dB.

Figure 8 shows the simulation and measurement result from Sierpinski carpet DGS LPF (Figure 6*d*). The simulation result shows that the cut off frequency occurs at 1.88 GHz with the insertion loss value at 0.1981 dB. While the measurement result shows that the cut off frequency is 1.819 GHz and the insertion loss value is 0.7863 dB. The discrepancy frequency is around 61 MHz.

Figure 9 shows the simulation and measurement result from Sierpinski carpet DGS LPF (Figure 6*e*). The simulation result shows that the cut off frequency occurs at 1.84 GHz with the insertion loss value is 0.3359 dB. While the measurement result shows that the cut off frequency is 1.728 GHz and the insertion loss value is 0.6481 dB. The discrepancy frequency is around 72 MHz.

Figure 10 shows the simulation and measurement result from Sierpinski carpet DGS LPF (Figure 6*f*). The simulation result shows that the cut off frequency occurs at 2 GHz with the insertion loss value is 0.219 dB. While the measurement result shows that the cut off frequency is 2 GHz and the insertion loss value is 1.663 dB. There is no discrepancy frequency, but the insertion loss value decreases.

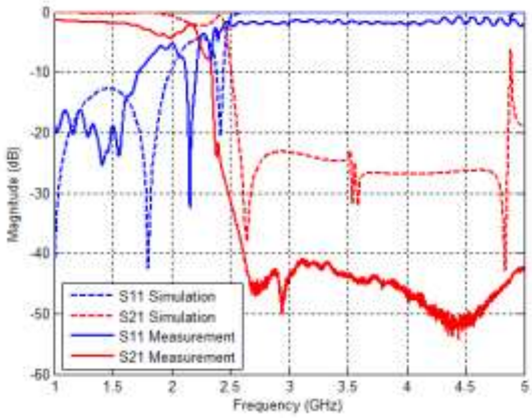

Figure 7. The simulation and measurement result from the HCR DGS LPF design. The dash line is the simulation and the solid line is the measurement result

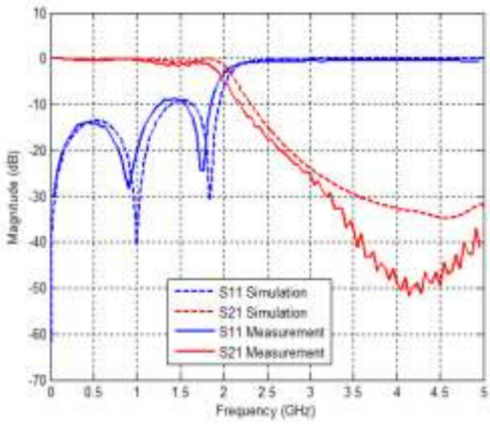

Figure 8. The simulation and measurement result for two steps of the Sierpinski carpet DGS LPF design are shown in Figure 6*d*. The dash line is simulation and the solid line is the measurement result

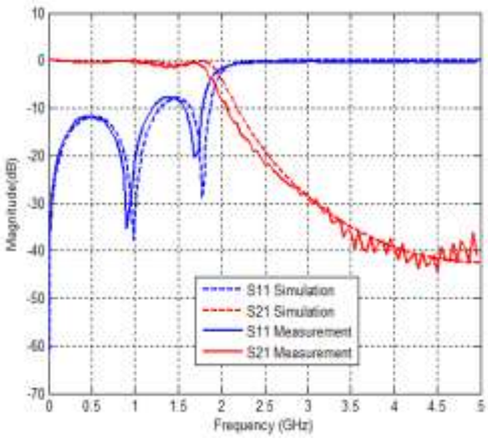

Figure 9. The simulation and measurement result for two steps of the Sierpinski carpet DGS LPF design are shown in Figure 6*e*. The dash line is simulation and the solid line is the measurement result

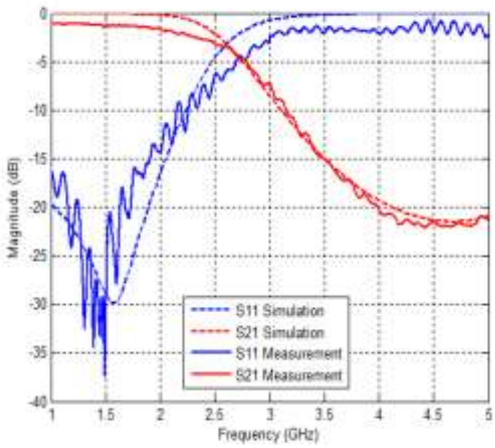

Figure 10. The simulation and measurement result for three steps of the Sierpinski carpet DGS LPF design are shown in Figure 6*f*. The dash line is simulation and the solid line is the measurement result

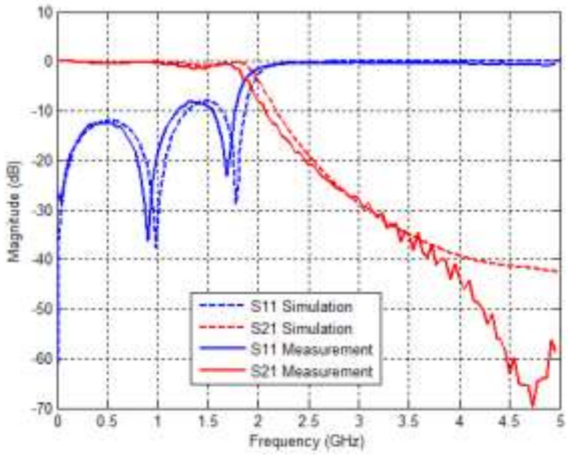

Figure 11. The simulation (dash line) and measurement (solid line) result for three steps of the Sierpinski carpet DGS LPF design are shown in Figure 6*g*

Figure 11 shows the simulation and measurement result from Sierpinski carpet DGS LPF as shown in Figure 6*g*. The simulation result shows that the cut off frequency occurs at 1.82 GHz and the insertion loss value is 0.2081 dB. While from the measurement result shows that the cut off frequency is 1.728 GHz and the insertion loss value is 0.682 dB. The discrepancy frequency is around 92 MHz. Table 1 describes the comparative study of the performance of proposed design with that already existing mentioned [9-22].

Table 1. Comprison performance of lowpass filters

Ref. No	Relative Dielectric Constant/Thickness of Dielectric	Cut-off Frequency	Stop-band	Note
[9]	9.6/0.8 mm	3 GHz	23 dB at 3.76 to 7.55 GHz	
[10]	2.2/31 mil	1.3 GHz	20 dB at 4.25 to 10 GHz	T Junction
	2.2/31 mil	1.3 GHz	20 dB at 3.8 to 8 GHz	Cross-junction
[11]	3.48/30 mil	2 GHz	15 dB at 3 to 5 GHz	
[12]	3.48/30 mil	2.5 GHz	20 dB at 4 to 10 GHz	
[13]	3.2/0.07 mm	2.4 GHz	20 dB at 2.55 to 4 GHz	
[14]	3.2/0.787 mm	4 GHz	30 dB at 5.17 to 10 GHz	
[15]	2.65/1.5 mm	2.5 GHz	20 dB at 2.7 to 7 GHz	
[16]	2.2/0.381 mm	1.96 GHz	10 dB at 2.4 to 8 GHz	
[17]	3.38/0.813 mm	2.4 GHz	20 dB at 2.95 to 8.25 GHz	
[18]	10/1.575 mm	3.6 GHz	20 dB at 4 to 7 GHz	
[19]	3.38/0.762 mm	3 GHz	40 dB at 4 to 9 GHz	
[20]	2.65/1.5 mm	2.25 GHz	30 dB at 2.4 to 5.5 GHz	
[21]	2.2/0.78 mm	2.15 GHz	20 dB at 2.4 to 25 GHz	
[22]	2.2/0.787 mm	5 GHz	20 dB at 5.5 to 14 GHz	
This Work	2.33/0.787 mm	2.173 GHz	40 dB at 2.62 to 5 GHz	HCR DGS
		1.728 GHz	20 dB at 2.5 to 5 GHz	Sierpinski Carpet DGS

5. Conclusion

In this research, defected ground structrure gives good performance for selectivity of filters. The bandpass of Hilbert Curve Ring defected ground structure has sharper skirt than Sierpinski Carpet. There exists a discrepancy frequency so it causes the degradation transmission and reflection factor. This discrepancy is mostly due to displacement figure simulation to prototype figure during the fabrication process. In addition the discrepancy is also caused by the effects of SMA connector.

References

[1] Mudrik Alaydrus, Dian Widiastuti, Teguh Yulianto. *Designing Cross-Coupled Bandpass Filter with Transmission Zeros in Lossy Microstrip*. IEEE International Conference on Information Technology and Electrical Engineering. Yogyakarta. 2013; 277-280.

[2] Dian Widi Astuti, Juwanto, Mudrik Alaydrus. *A Bandpass Filter Based on Square Open Loop Resonator at 2.45 GHz*. IEEE International Conference on Instrument, Communications, Information Technology and Biomedical Engineering. Bandung. 2013; 147-151

[3] Wen Chen, Yongjiu Zhao, Zhouxiao Jun. Compact and Wide Upper-Stopband Triple-Mode Broadband Microstrip BPF. *TELKOMNIKA (Telecommunication, Computing, Electronics and Control).* 2012; 10(2): 353-358.

[4] Fajri Darwis, Arief Budi Santiko, Novita Dwi Susanti. Design of Compact Microstrip U Shape Bandpass Filter using Via Ground Holes. *TELKOMNIKA (Telecommunication, Computing, Electronics and Control).* 2016; 14(1): 82-85.

[5] Yatindra Gaurav, RK Chauhan. A Compact UWB BPF with a Notch Band using Rectangular Resonator Sandwiched between Interdigital Structure. *International Journal of Electrical and Computer Engineering (IJECE)*. 2017; 7(5): 2420-2425

[6] Jong-Sik Lim, Chul-Soo Kim, Jun-Seok Park, Dal Ahn, Sangwook Nam. Design of 10 dB 90° Branch Coupler using Microstrip Line with Defected Ground Structure. *Electronics Letters*. 2000; 36(21): 1784-1785.

[7] Jong-Sik Lim, Sung-Won Lee, Chul-Soo Kim, Jun-Seok, Park, Dal Ahn, Sangwook Nam. A 4:1 Unequal Wilkinson Power Divider. *IEEE Microwave and Wireless Components Letters*. 2001; 11(3): 124-126.

[8] Jong-Sik Lim, Young-Taek Lee, Jae-Hee Han, Jun-Seok Park, Dal Ahn, Sangwook Nam. *A Technique for Reducing the Size of Amplifiers Using Defected Ground Structure*. Proceedings of Microwave Symposium Digest, IEEE MTT-S Digest. Seatlle. 2002; 2: 1153-1156.

[9] JX Chen, JL Li, KC Wan, Q Xue. *Compact Quasi-Elliptic Function Filter Based on Defected Ground Structure*. IEE Proc-Microw. Antennas Propag. 2006; 153(4): 320-324.

[10] Dal Ahn, Jun-Seok Park, Chul-Soo. Kim, Juno Kim, Yongxi Qian, Tatsuo Itoh. A Design of The Low-Pass Filter using The Novel Microstrip Defected Ground Structure. *IEEE Transaction on Microwave Theory and Techniques*. 2001; 49(1): 86-93.

[11] Jong-Sik Lim, Chul-Soo Kim, Young-Taek Lee, Dal Ahn, Sangwook Nam. *A New Type of Low Pass Filter with Defected Ground Structure*. Proceedings of 32nd Eropean Microwave Conference. Milan. 2002;

[12] Jong-Sik Lim, Chul-Soo Kim, Dal Ahn, Yong-Chae Jeong, Sangwok Nam. Design of Low-Pass Filters using Defected Ground Structure. *IEEE Transactions on Microwave Theory and Techniques*. 2005; 53(8): 2539-2545.

[13] Arjun Kumar, Hossein Alavi, Jason A. Mix, Edgar Colin Beltran, Elizabeth Cruz Perez, Aline Jaimes Vera. *Design of Nine Pole Microstrip Low Pass Filter with Metal Loaded Defected Ground Structure*. Proceedings of IEEE MTT-S Latin America Microwave Conference. Puerto Vallarta, Mexico. 2016;

[14] XQ Chen, RL Li, SJ Shi, Q Wang, L Xu, XW Shi. A Novel Low Pass Filter using Elliptic Shape Defected Ground Structure. *Progress in Electromagnetics Research B*. 2008; 9: 117-126.

[15] Bian Wu, Bin Li, Changhong Liang. Design of Lowpass Filter Using A Novel Split-Ring Resonator Defected Ground Structure. *Microwave and Optical Technology Letters*. 2007; 49(2): 288-291.

[16] Mrinal Kanti Mandal, Subrata Sanyal. A Novel Defected Ground Structure for Planar Circuits. *IEEE Microwave and Wireless Components Letters*. 2006; 16(2): 93-95.

[17] Jinping Yang, Wen Wu. Compact Elliptic-Function Low-Pass Filter Using Defected Ground Structure. *IEEE Microwave and Wireless Components Letters*. 2008; 18(9): 578-580.

[18] M Kufa, Z. Raida. Lowpass Filter with Reduced Fractal Defected Ground Structure. *Electronics Letters*. 2013; 49(3).

[19] H Liu, Z Li, X Sun. Compact Defected Ground Structure in Microstrip Technology. *Electronics Letters*. 2005; 41(3).

[20] J Chen, ZB Weng, YC Jiao, FS Zhang. Lowpass Filter Design of Hilbert Curve Ring Defected Ground Structure. *Progress in Electromagnetics Research*. 2007: 269-280.

[21] He-Xiu Xu, Guang-Ming Wang, Chen-Xin Zhang, Qing Peng. Hilbert-Shaped Complementary Single Split Ring Resonator and Low-Pass Filter with Ultra-Wide Stopband, Excellent Selectivity and Low Insertion-Loss. *International Journal of Electronics and Communications*. 2011; 65: 901-905.

[22] Zhang wei, Yang Wei-ming, Fang yin-yin, Hu Cheng-kang, Zhu Xing-yu, Ma ge. *Design of the Hilbert Fractal Defected Ground Structure Low-pass Filter*. IEEE International Conference on Communication Problem-solving. Beijing. 2014: 99-102.

[23] MA Kenari, MN Moghadasi, RA Sadeghzadeh, BS Virdee, E. Limiti. Dual-band RFID Tag Antenna Based on The Hilbert-Curve Fractal for HF and UHF Applications. *IET Circuits Devices & System*. 2016; 10(2): 140-146.

[24] P Lande, D Davis, N Mascarenhas, F Fernandes, A Kotrashetti. Design and Development of Printed Sierpinski Carpet, Sierpinski Gasket and Koch Snowflake Fractal Antennas for GSM and WLAN

Applications. IEEE International Conference on Technologies for Sustainable Development. Mumbai. 2015;
[25] Nordalyana Murni Fadzil, Shipun Anuar Hamzah, Abdirahman Mohamud Shire, Khairun Nidzam Ramli, Fauziahanim Che Seman, Mazlina Esa, Nik Noor Nik Abd Malik. *Sierpinski Carpet Fractal Antenna with Harmonic Suppression Capability*. IEEE International Conference on Computer and Communication Engeneering. Kuala Lumpur. 2016: 392-395.
[26] RJ Chitra, V Nagarajan. *Design and Development of Koch Fractal Antenna.* IEEE International Conference on Communication and Signal Processing. 2016; 2294-2298.
[27] A Bakythekov, AR Maza, M Nafe, A.Shamim. *Fully Inkjet Printed Wide Band Cantor Fractal Antenna for RF Energy Harvesting Application.* IEEE European Conference on Antennas and Propagation. 2017; 489-491.
[28] Mudrik Alaydrus. Hybrid Methods in Designing Sierpinski Gasket Antennas. *TELKOMNIKA (Telecommunication, Computing, Electronics and Control)*. 2010. 8(3): 225-234.
[29] Mudrik Alaydrus. *Comparison of Several Hybrid Methods in Analyzing Sierpinksi Gasket Antennas with Finite Ground*. IEEE Asia-Pacific Conference on Applied Electromagnetics. Malaysia.2010
[30] SC Patricio, M Carleti, A Cerqueira S Jr, JAJ Ribeiro. *Development of a Printed Antenna Array based on Sierpinski Carpet Fractal Elements.* IEEE MTT-S International Microwave and Optoelectronics Conference. Porto de Galinhas. 2015: 1-6.
[31] Icaro V Soares, Ursula C Resende, Sandro TM Goncalves. *Sierpinski Carpet Fractal Microstrip Arrays for Energy Harvesting Applications*. IEEE Conference on Electromagnetic Field Computational. Miami. 2016: 1-1.
[32] AF Morabito, AR Laganà, G Sorbello, T Isernia, Mask-Constrained Power Synthesis of Maximally Sparse Linear Arrays through A Compressive-Sensing-Driven Strategy.*Journal of Electromagnetic Waves and Applications*. 2015; 29(10): 1384-1396.
[33] AF Morabito, AR Lagana, T Isernia. Isophoric Array Antennas with A Low Number of Control Points: a 'size tapered' solution. *Progress in Electromagnetics Research Letters*. 2013; 36: 121-131.
[34] Yaqeen S Mezaal, Halil T Eyyuboglu, Jawad K Ali. *New Dual Band Dual-Mode Microstrip Patch Bandpass Filter Designs Based on Sierpinski Fractal Geometry*. IEEE Third International Conference on Advanced Computing & Communication Technologies. Rohtak. 2013: 348-352.
[35] Yaqeen S Mezaal. A New Microstrip Bandpass Filter Design Based on Hilbert Fractal Geometry for Modern Wireless Communication Applications. *International Journal of Advancements in Computing Technology*. 2009; 1(2): 35-39.
[36] Yaqeen S Mezaal, Halil T Eyyuboglu, Jawad K Ali. Wide Bandpass and Narrow Bandstop Microstrip Filters Based on Hilbert Fractal Geometry Design and Simulation Results. *PLoS ONE*. 2014: 1-15.
[37] Jia-Sheng Hong. Microstrip Filters for RF/Microwave Application. Second Edition. New Jersey: John Wiley & Sons. 2011: 112-115.